A criterion for the pinning and depinning of an advancing contact line on a cold substrate

Rémy Herbaut, Julien Dervaux, Philippe Brunet, Laurent Royon, Laurent Limat

Eur. Phys. J. Special Topics **229**, 1867–1880 (2020)

https://doi.org/10.1140/epjst/e2020-900261-5

THE EUROPEAN PHYSICAL JOURNAL SPECIAL TOPICS

Regular Article

A criterion for the pinning and depinning of an advancing contact line on a cold substrate

Rémy Herbaut[1,2,a], Julien Dervaux[1], Philippe Brunet[1,b], Laurent Royon[2], and Laurent Limat[1]

[1] Université de Paris, Laboratoire Matière et Systèmes Complexes, UMR 7057 CNRS, 75013 Paris, France
[2] Université de Paris, Laboratoire Interdisciplinaire des Energies de Demain, UMR 8236 CNRS, 75013 Paris, France

Received 2 November 2019 / Accepted 6 July 2020
Published online 14 September 2020

Abstract. The influence of solidification on the spreading of liquids is addressed in the situation of an advancing liquid wedge on a cold substrate at $T_p < T_f$, where T_f is the melting temperature, and infinite thermal conductivity. We propose a model of contact-line dynamics derived from lubrication theory, where equilibrium between capillary pressure and viscous stress is at play. Here it is adapted to a quadruple line geometry, where vapour, liquid, frozen liquid and basal substrate meet. The Stefan thermal problem is solved in an intermediate region between molecular and mesoscopic scales, allowing to predict the shape of the solidified surface. The apparent contact angle versus advancing velocity U takes a minimal value, which is set as the transition from continuous advancing to pinning. We postulate that this transition corresponds to the experimentally observed critical velocity, dependent on undercooling temperature $T_f - T_p$, below which the liquid is pinned and advances with stick-slip dynamics. The analytical solution of the model shows a qualitatively fair agreement with experimental data, and the best agreement is obtained from the adjustment of a mesoscopic cut-off length as fitting parameter. We discuss of the dependence of this cut-off length on T_p

1 Introduction

Contact line dynamics is a still challenging problem motivating many studies. The multi-scale nature of the problem, the existence of several conflicting models, combined with the difficulty to obtain exhaustive and reproducible data has left this problem still open [1–3]. Of special difficulty is the case in which the contact line motion is combined with phase change, like for instance evaporation/condensation of the liquid [4–7], colloids or particles deposition [8–11], or solidification of a liquid moving on a cold substrate [12–17]. In this latter case, as well as in that of colloid

[a] e-mail: remy.herbaut@univ-paris-diderot.fr
[b] e-mail: philippe.brunet@univ-paris-diderot.fr

deposition [8], it is observed that the continuous advancing or receding of a contact line can be interrupted when one reduces the velocity U down to a threshold U_c for contact line pinning [16], below which stick-slip behaviour can be observed as well [14,17]. Understanding these phenomena is of crucial importance for several applications, including 3D printing [18], or aircraft icing [19].

To account for this transition, models are still lacking. Schiaffino and Sonin [12,13,16] developed what can be understood as a "four phases" contact line model (substrate, air, liquid, frozen liquid) that they carried out numerically. Their peculiar situation was that of a thin liquid layer, fed from successive impacting droplets, and spreading on an already frozen solid base formed on the cold substrate. A difficulty that they noticed is that, just as the same way as the evaporation rate for colloid deposition ("coffee stain" problem) [20,21], a divergence of heat flux appears near the contact line, which should similarly imply a divergence of solid freezing rate. The liquid layer flowing above the basal solid deposit then should freeze much faster than the characteristic time of the flow. This singularity has led the authors to introduce a mesoscopic cut-off length in the micron range, of yet unknown origin. In view of these problems, Tavakoli et al. [14] postulated a different structure for the solid/liquid interface. In this quasi-static approach, the interface should correspond to an isotherm and would intersect the liquid/air interface with a right angle - based on the assumption that the thermal flux is negligible within the vapour phase [22]. The equilibrium is supposed to be broken when the total deposited volume remains below some threshold. The agreement with experiments is fair, but the threshold volume is an unknown, empirically adjusted parameter. Furthermore, the question of how the liquid flows at higher velocity remains elusive and unspecified in this approach. Another way to tackle the problem has been proposed by de Ruiter et al. [15], and consists in admitting some lag in solidification, denoted as kinetic undercooling, that depends on the contact line velocity. This leads to a critical temperature in the vicinity of the contact line, below which the liquid locally freezes. This should lead to the arrest of the spreading in agreement with experiments [15]. This feature was also reproduced with thermoresponsive polymer solutions [23] on hot substrates. Let us note that the experiments did not exhibit stick-slip dynamics, as the liquid was not continuously forced to spread on the substrate [15]. Another difficulty of the subject is a lack of a model that could give elements for a semi-quantitative analysis, in a way similar to a model of advancing contact-line or "a la Voinov", i.e. a hydrodynamical framework in the lubrication approximation [24].

In the present paper, we aim to build such a framework while trying to reconcile the aforementioned three approaches. We consider a four-phases contact line advancing on a cold plate of infinite thermal conductivity (see Fig. 1). The angles $\theta_s(x)$ and $\theta_L(x)$ respectively stand for the angle formed by the solid with the substrate and by the liquid/air interface with the horizontal. These two angles are expected to (slowly) depend on the horizontal coordinate x. We assume total wetting conditions of the liquid on the solid phase ($\theta_e = \theta_L - \theta_s = 0$ for $U = 0$), and interfaces with small slope so that lubrication approximation can be applied. Let us here note that the liquid-on-solid equilibrium angle can be nonzero for liquid water on ice [25], where values around 10° were measured. This is presumably due to the peculiar molecular structures of liquid water and ice. Though, the assumption θ_e shall be acceptable for most liquids, in particular for low-surface energy alcanes for which experiments are available. We assume that at a certain mesoscopic scale, thereafter denoted as b, there is a crossover between the first two aforementioned approches and we develop a simple model deduced from Voinov's theory [24], completed with a Stefan kinetic condition at the solid/liquid front. The microscopic length scale is denoted as the cut-off length a, and shall be considered as the molecular size. A steady solution for this four phases contact line can exist only if a specific condition is set between the advancing velocity and the speed of the solid-liquid front. Our study investigates this

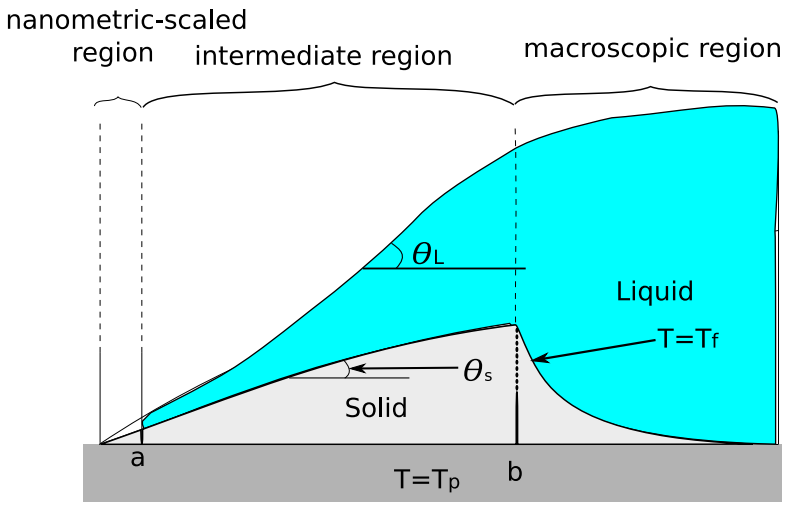

Fig. 1. Sketch of the quadruple line geometry, combining Schiaffino & Sonin's [12,13,16] and Tavakoli et al.'s [14] approaches. Let us note that the curvature of the free-surface (due interface bending induced by viscous shear stress) and the curvature of the solid-liquid front, have opposite signs.

condition of existence. Let us note that the case of supercooled liquids is not considered in this study. This would involve a delay in solidification, especially within the range where the substrate temperature is close to the freezing one [26].

We first describe the equations of the model (Sect. 2.1), then we show the main predictive plots (Sect. 2.2), and finally we discuss on the limitations of the model, the physical meaning of the cut-off length b and the importance of its adjustment, and we finally conclude on the prospectives.

2 A quadruple dynamical contact-line

Let us consider a liquid wedge (density ρ, viscosity η and surface tension γ) in contact with a substrate of temperature T_p smaller than the melting temperature T_f, so that liquid is partially frozen along the contact area with the substrate. We focus on the vicinity of the contact-line, hence in a typical situation of a moving sessile drop or a climbing meniscus. For sake of simplicity, we adopt here a two-dimensional (2D) geometry.

We assume that the liquid and solid wedges, of angles respectively equal to $\theta_L - \theta_s$ and θ_s, are in contact with each other and form altogether an apparent contact angle θ_L with the substrate, which holds until the nanometric scale, see Figure 1. Let us assume a steady situation where both wedges advance at the same velocity U with respect to the substrate. This condition of steadiness shall impose a relationship between the line velocity and the liquid-solid front dynamics.

We also assume total wetting condition ($\theta_e = 0$ for $U = 0$) and a steady advancing contact-line, i.e. U remains constant and positive. As set in Figure 1, the solid/liquid wedge is divided into three distinct domains:

- a nanometer-scale region ($x < a$) of molecular size,
- an intermediate mesoscopic region ($a < x < b$) defining the quadruple contact line, where the free-surface, the liquid/solid and the solid/substrate interfaces co-exist. It is in this region that viscous shear stress develops,

– a macroscopic quasi-static region ($x > b$) where the solidification front corresponds to the isotherm $T = T_f$ in the liquid bulk.

The substrate temperature is kept constant at $T_p < T_f$, which is assumed to be uniform. This assumption is valid if the substrate thermal conductivity κ_P is large enough. The approach of dynamical contact-lines proposed within the intermediate region is inspired from the hydrodynamic model of Voinov [24].

Let us finally underline that the sketch of Figure 1 is of course an oversimplification of the real solid-liquid front profile. However, it suggests that:

– in the macroscopic domain, the front is ruled by a classical Stefan problem at thermal equilibrium where, due to the negligible conduction of the ambient air, the $T = T_f$ isotherm has to be normal to the fluid free-surface,

– in the mesoscopic domain, the front is out of equilibrium and is ruled by a balance between thermal conduction, viscous shear stress and capillary forces near the contact-line. This is the domain investigated in our model. The sudden change of slope of the solid profile, which is possibly less sharp in reality, reflects this crossover.

2.1 Model of contact line dynamics a la Voinov with solidification

2.1.1 Voinov model in the intermediate region

Shear stress coupled to capillary forces at the contact-line induces what is commonly denoted as viscous bending, a framework classically used to predict the dynamics of triple contact lines in the hydrodynamical context [1,2,24]. This viscous shear has no reason to be uniform within the whole wedge and generally depends on x [1,2]. Hence, the curvature of the free-surface and that of the liquid/solid interface are supposedly nonzero and taken into account.

The liquid region forms an angle $\theta_L - \theta_s$ advancing with the solid front. A steady state situation ($U = \text{cte}$) like that depicted in Figure 2 is possible only if it is assumed that the liquid free-surface and liquid/solid interface advance at the same velocity U (that of the quadruple line), so that the interface adopts a steady shape in the moving frame. This condition of existence thus implies a condition relating U and the solid/liquid front dynamics at any $x > 0$, which itself depends on the wedge geometry.

A flow is established in the liquid wedge of height $h_l(s)$, s being the coordinate along the solid front. In our case, the curvature of the solid front is assumed to be small - i.e. its radius of curvature is much larger than the mesoscopic length b, along this wedge. This yields a continuity equation:

$$\frac{\partial h_l}{\partial t} = \frac{\partial (h_l \langle u \rangle)}{\partial s} = U \cos\theta_s \frac{\partial h_l}{\partial s}, \tag{1}$$

where $\langle u \rangle$ is the average velocity in the liquid, slowly varying with s, that approximately reads:

$$\langle u \rangle \simeq \frac{\gamma h_l^2}{3\eta} \frac{\partial^3 \xi}{\partial s^3},$$

where $y = \xi(s)$ denotes the profile of the free-surface.

We also define U_s as being the front velocity, in the direction perpendicular to the solid/liquid front, and similarly we get $U_s = U \sin\theta_s$.

The slope of the interfaces remains small ($\theta_L \ll 1$ and $\theta_s \ll 1$). Under these assumptions, we can assume that $\cos\theta_s \simeq 1$ in equation (1) and we replace $\frac{\partial^3 \xi}{\partial s^3}$ by $\frac{\partial^3 h_l}{\partial s^3}$, which yields the classical equation [27]:

$$\frac{\partial^3 h_l}{\partial s^3} \simeq 3\frac{Ca}{h_l^2}, \tag{2}$$

where $Ca = \frac{\eta U}{\gamma}$ stands for the dimensionless capillary number. Also with $\theta_e = 0$, this equation leads to the well-known Tanner solution that gives the angle $\theta_L(s)$ at the distance s from the corner:

$$\Big(\theta_L(s) - \theta_s(s)\Big)^3 \simeq 9\ Ca \log\frac{s}{a}. \tag{3}$$

The determination of θ_s involves a balance in thermal flux, which must be considered in order to predict the complete evolution of θ_L with U.

Let us note that the validity of the usual hydrodynamic equations, commonly set on a straight substrate, and considered here on a slightly curved solid, implies that the solid radius of curvature be weak compared to the value of b, in order that the previous equations remain valid at first order. This assumption is to be checked later in the paper, and we shall show that it is generally true, providing one pays attention on the choice of b.

2.1.2 Thermal equilibrium in the wedge

We assume an infinite thermal conductivity of the substrate, and also the heat transfer between liquid and the ambient atmosphere is assumed to be negligible. Considering these assumptions, the heat flux is dominated by conduction within the solid wedge. The heat flux generated across the liquid-solid interface by the substrate at T_p, rules the solid angle θ_s within the liquid wedge. This flux is determined by the heat equation, which in a steady situation where convection is neglected, reads as the classical Laplacian equation:

$$\nabla^2 T(r,\phi) = 0. \tag{4}$$

Equation (4) is solved in a wedge of angle $\theta_s(x)$ at any $x > 0$, with $T = T_p$ and $T = T_f$ respectively as boundary conditions along the horizontal substrate/solid interface and along the solid/liquid interface, for any $x > 0$. The Laplacian equation is solved in polar coordinates with radial and angular spatial variables r and ϕ represented in Figure 2.

Applying the classical separation of variables, the resolution of equation (4) yields:

$$T(r,\phi) = \mathcal{F}(r)\mathcal{G}(\phi) = (a_0 + b_0 \ln r)(A_0 + B_0\phi) + (\alpha r^{\upsilon} + \beta r^{-\upsilon})(A\cos(\upsilon\phi) + B\sin(\upsilon\phi)), \tag{5}$$

where a_0, b_0, A_0, B_0, α, β, A and B are constants. The following boundary conditions allow us to determine the constants:

$$T(r,0) = T_p \ \text{ and } \ T(r,\theta_s) = T_f. \tag{6}$$

We set $\Delta T = T_f - T_p > 0$ as the main control parameter of this thermal problem. The temperature remains finite in the vicinity of the corner, so that $\beta = 0$. It yields

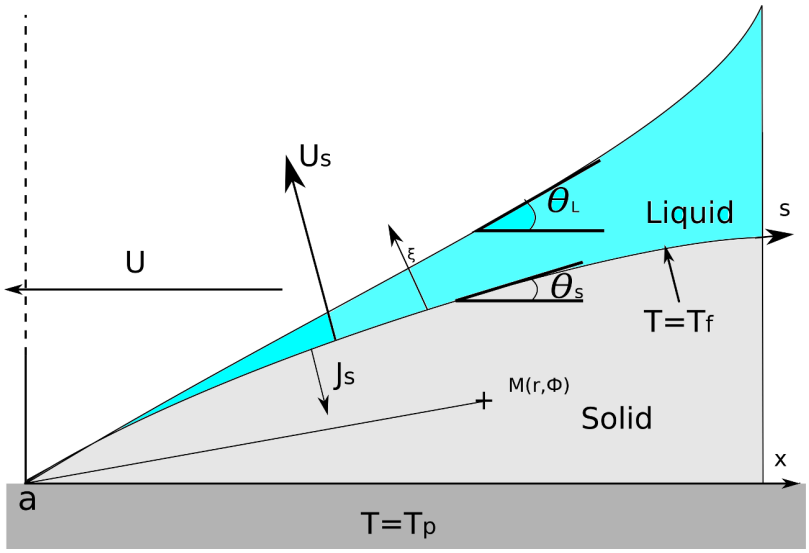

Fig. 2. Zoomed sketch of the quadruple line within the intermediate region, with the continuous hydrodynamic approach by Voinov [24], i.e. a finite and spatially dependent curvature of the film and solid front, to rule the visco-capillary balance in the liquid. The figure also shows the sketch of the thermal Stefan problem in the wedge.

a general expression for the solution of equation (5):

$$T(r,\phi) = T_p + \left(\frac{\Delta T}{\theta_s}\right)\phi + \sum_{n=1}^{\infty} \alpha_n r^{\frac{n\pi}{\theta_s}} \sin\left(\frac{n\pi\phi}{\theta_s}\right). \tag{7}$$

In the simpler situation of a solid wedge forming a constant angle θ_s, the solution of the temperature field $T(r,\phi)$ would only contain lowest order terms, and would express as:

$$T_0(r,\phi) = T_p + \left(\frac{\Delta T}{\theta_s}\right)\phi. \tag{8}$$

Our present situation is that of a (weakly) curved solid/liquid interface, i.e the wedge angle θ_s is weakly dependent on x (or r). To account for this higher order correction, let us introduce the small parameter ϵ such that $\theta_s = \theta_s(\epsilon r)$. We now seek for a solution of the stationary diffusion equation (4) for the temperature of the form:

$$T(r,\phi) = T_p + \left(\frac{\Delta T}{\theta_s(\epsilon r)}\right)\phi + \epsilon T^1(r,\phi). \tag{9}$$

After injecting the equations (9) into (4) and (6) and expanding in powers of ϵ, we obtain the following solution up to zeroth order in ϵ:

$$T(r,\phi) = T_p + \frac{\Delta T}{\theta_s(0)}\phi - \epsilon r \frac{\Delta T \theta_s'(0)\sin\phi}{\theta_s(0)\sin\theta_s(0)}. \tag{10}$$

Let us recall that the flux across the liquid-solid interface is:

$$J_s(s, \phi = \theta_s) = -\frac{\kappa}{s}\frac{\partial T}{\partial \phi} = \kappa \frac{\Delta T}{s\theta_s}, \tag{11}$$

where κ stands for the thermal conductivity of the solid. This heat flux rules the Stefan condition at the interface, which progresses at velocity U_s, and is related to the advancing velocity U. This enables us to determine the solidification front kinetics from (11):

$$J_s(s, \phi = \theta_s) = \rho L U_s = \rho L U \sin\theta_s, \tag{12}$$

where L stands for the liquid/solid latent heat. This flux through the liquid/solid interface can be evaluated from a simple integration of equations (11) and (12), under the assumptions of small angle and small curvature.

Back to equation (10), we obtain in the limit of small angles:

$$\frac{\kappa\Delta T}{s\theta_s(0)} - \epsilon\frac{\kappa\Delta T\theta_s'(0)}{\theta_s(0)^2} = \rho L U \theta_s(\epsilon r), \tag{13}$$

which, from a formal identification at the zeroth order in ϵ, yields:

$$\frac{\kappa\Delta T}{s\theta_s(\epsilon s)} = \rho L U \theta_s(\epsilon s). \tag{14}$$

The solution of equation (14) above is reduced to:

$$\theta_s(s) = \left(\frac{\kappa\Delta T}{\rho L U s}\right)^{\frac{1}{2}}. \tag{15}$$

Let us note that under the assumption of $\theta_s \ll 1$, and assuming small enough curvature, in what follows we can substitute the curvilinear coordinate s by x in equation (15).

2.1.3 The dependence of θ_L on U yields a transition to unstable dynamics

Returning to the Voinov-Tanner equation (3), an expression for the apparent dynamical contact angle θ_L reads:

$$\theta_L(x) = \left(\frac{\kappa\Delta T}{\rho L U x}\right)^{\frac{1}{2}} + \left(9\, Ca \log\frac{x}{a}\right)^{\frac{1}{3}}. \tag{16}$$

Thus, θ_L depends on the substrate temperature T_p – i.e. on the undercooling offset ΔT, and on the advancing velocity U.

Figure 3a shows θ_L versus U from equation (16), for various ΔT and a value of the mesoscopic length $x = b$ set at 1 μm. We took values for solid and liquid hexadecane, for which $\rho = 833$ kg.m^{-3}, $\kappa = 0.15$ W.m^{-1}.K^{-1}, $L = 2.3 \times 10^5$ J.kg^{-1}, $\eta = 3 \times 10^{-3}$ Pa.s, $\gamma = 0.028$ N.m^{-1} and $a = 0.845$ nm.

Let us note that the model is surely not valid as U approaches zero. Actually, our framework is based on that when $U < U^*$, the solid front moves faster than the

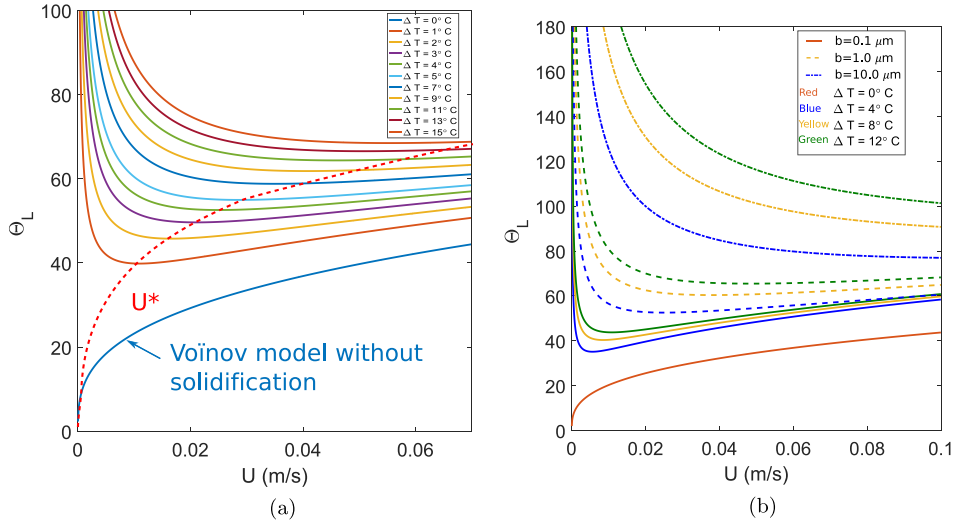

Fig. 3. (a) Apparent advancing angle θ_L versus advancing velocity U and various values of ΔT ($a = 0.845$ nm (molecular size) and $x = b = 1$ μm). Except in the isothermal case, θ_L shows a minimum for a critical velocity U^*, which is taken as the value for the transition to unsteady dynamics. (b) Same as (a) but with different values of b and ΔT.

advancing contact-line. Therefore, the dynamics becomes unstable (in experiments, it corresponds with the appearance of stick-slip) and our framework of steady solid front and liquid wedge is not valid anymore. Therefore the divergence of θ_L as U tends to 0 then reflects the mechanism related to the model, namely that the solidification induces the pinning of the contact line.

Let us also note that for $\Delta T = 0$, the angle θ_s equals zero, and that we retrieve the isothermal situation. For $\Delta T > 0$, hence in the situation of partial solidification of the liquid, the evolution of θ_L for relatively large U follows a trend similar to the isothermal situation, with an increase of θ_L with U. However, at relatively low velocity, i.e. below a critical velocity ($U < U^*$), our model predicts a sharp decrease of θ_L with U. Therefore, our model leads to a non-monotonous dependence of θ_L upon U. We emphasize the fact that θ_L is the apparent contact angle of the liquid, i.e. the slope of the liquid-air interface with respect to the cold substrate, while the relative slope with respect to the formed solid $\theta_L - \theta_s$ is much smaller and reduces to Voinov solution without solidification displayed on the same figure. In consistence with the lubrication assumptions, this relative angle remains small enough, and is here smaller than 40°.

Figure 3b shows θ_L versus U for different sets of values for b and ΔT. Clearly the value of $x = b$ strongly influences the location of U^*. Comparisons with existing experiments, to be shown later, will enable to better justify the choice of $b = 1$ μm.

At this stage, we state that the existence of a minimum for $\theta_L(U)$ implies an unstable situation from a mechanical point of view. Let us here remind the general expression of the capillary motile force, here expressed per unit length of contact-line, from the unbalanced Young's equation:

$$F_{\text{cap}} = \gamma\pi(\cos\theta_e - \cos\theta_L) \simeq \gamma\pi\left(\frac{\theta_L^2}{2} + \frac{\theta_L^4}{24}\right). \tag{17}$$

In a steady situation $U = $ cte, this capillary force is usually balanced by a viscous friction force $F_v \sim \eta U$ originating from shear stress within the wedge between

microscopic and macroscopic scales. Keeping the first order term in the development, it yields:

$$F_v \sim \gamma\pi\left(\frac{\theta_L^2}{2}\right). \tag{18}$$

The fact that F_v [N.m^{-1}] be proportional to θ_L^2, means that the liquid/substrate friction decreases with velocity in the domain $U < U^*$. Intuitively, when a higher U leads to a smaller friction force F_v (here expressed per unit length), the situation is dynamically unstable. Therefore, in analogy with solid friction [28,29], we postulate that this decreasing branch is unstable and can lead to stick-slip dynamics below some critical velocity U^*. We then assume that U^* corresponds to the location of the minimum of $\theta_L(U)$, which delimitates the transition between continuous and stick-slip dynamics. Therefore, this framework allows us to analytically calculate an estimate for U^* and for the related critical (apparent) contact angle $\theta_L^* = \theta_a$.

2.2 Prediction of critical velocity and arrest angle

The minimum of the apparent angle with U is given by $\dfrac{\partial\theta_L}{\partial U}(U^*) = 0$, determined from equation (16). The resulting critical velocity reads:

$$U^* = \left(\frac{3}{2}\right)^{\frac{6}{5}}\left(\frac{6\eta}{\gamma}\log\frac{b}{a}\right)^{-\frac{2}{5}}\left(\frac{k\Delta T}{\rho L b}\right)^{\frac{3}{5}}. \tag{19}$$

We note that U^* follows a scaling law with the undercooling temperature: $U^* \sim \Delta T^{\frac{3}{5}}$. As underlined in Figure 3, the cut-off length b, which is an adjustable parameter of our model, has significant influence on U^*. Figures 4a and 4b show typical trends of U^* versus ΔT, for various values of b from 0.15 to 9 μm. A larger b tends to decrease the critical velocity, for the same ΔT. In other terms, the range of stability is wider in velocity for smaller values of b.

A prediction for the critical apparent angle θ_a is obtained by combining equations (16) and (19):

$$\theta_a = \left(\left(\frac{3}{2}\right)^{-\frac{3}{5}} + \left(\frac{3}{2}\right)^{\frac{3}{5}}\right)\left(\frac{9\eta\kappa\Delta T}{\gamma\rho L b}\log\frac{b}{a}\right)^{\frac{1}{5}}. \tag{20}$$

The predictions for θ_a versus ΔT, given by equation (20), are plotted in Figure 5. We assume that the determination of the apparent angle is carried out at a distance of the quadruple line equal to the mesoscopic length $r = b$. In Figure 5, the value of b is varied from 0.01 to 9 μm, hence within a range extended to smaller values compared to Figure 4.

Schiaffino and Sonin [16] theoretically determined mesoscopic cut-off lengths for wax paraffine (denoted there as λ) and proposed temperature-dependent values. For instance, for $\Delta T \simeq 7\,^\circ$C, $\lambda = 0.77$ μm, and for $\Delta T \simeq 34\,^\circ$C, they found $\lambda = 0.12$ μm. Since the length λ has a similar physical meaning as our parameter b, we are confident that our choice for the range of b is realistic.

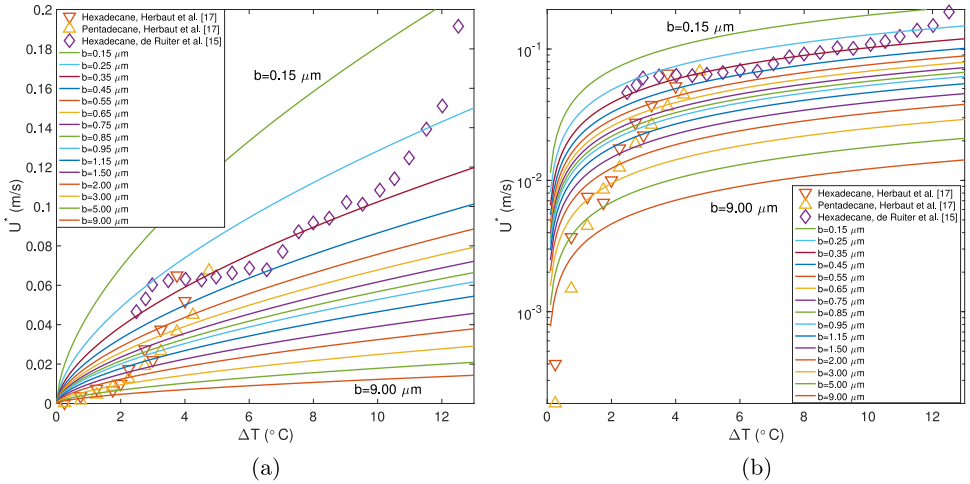

Fig. 4. (a) Critical velocity versus ΔT, for different values of b. Data points are experiments from de Ruiter et al. [15] and Herbaut et al. [17]. (b) Same as (a) in Semilogarithmic axes.

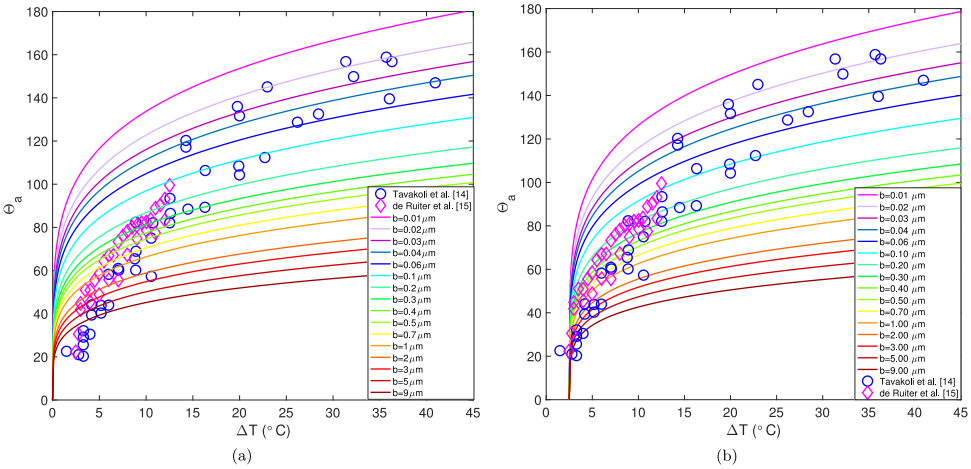

Fig. 5. (a) Apparent angle θ_a of liquid on substrate, versus undercooling ΔT, predicted by equation (20). The different curves correspond to different values of the mesoscopic cut-off length b, (a is set to 0.845 nm). Data points are experiments from de Ruiter et al. [15] and from Tavakoli et al. [14]. (b) Same as (a) with an offset in temperature added in equation (20), $\Delta T_c = 2.46°$.

2.3 Comparison with existing experiments

2.3.1 Critical velocity and its relationship to spreading arrest condition

First, let us remark that our model gives a criterion for the existence of a steady dynamics for an advancing quadruple line, which is based on a temperature-dependent critical advancing velocity. This is to be related to recent experiments by de Ruiter et al. [15] and Herbaut et al. [17].

In Figures 4 and 5, we inserted data points from different experiments of previous studies, to be compared with the results of the model. Let us first comment on how

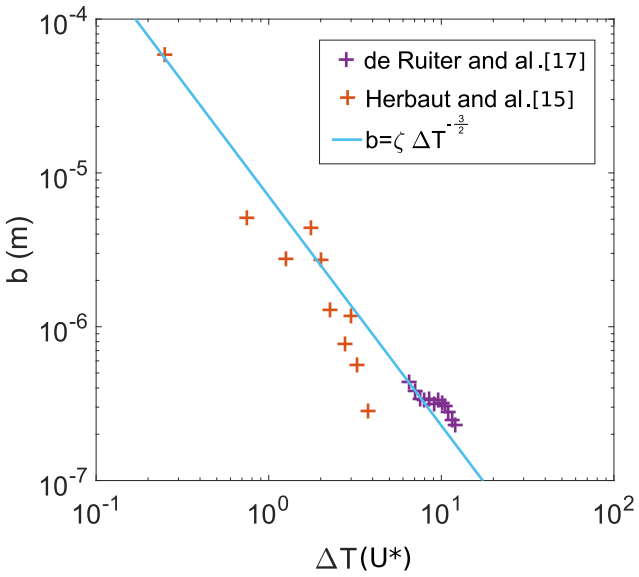

Fig. 6. Mesoscopic cut-off length b versus the critical temperature $\Delta T^*(U^*)$, with U^* being the critical velocity obtained from de Ruiter et al. [15] and Herbaut et al. [17]. The value for the prefactor is $\zeta = 7.053\ 10^{-6}$ m.K$^{-\frac{3}{2}}$.

these data were obtained. The critical velocity U^* was extracted from experiments of a single drop spreading on a cold substrate [15], and of a liquid bridge driven on a cold substrate put on a translation stage at constant velocity [17]. In both cases, $U^*(\Delta T)$ corresponds to the limit velocity below which the liquid on a substrate at $T_p = T_f - \Delta T$ stops spreading and gets its contact-line pinned. In [17], it corresponds to the occurrence of a stick-slip dynamics. In our model, it may correspond to the limit of the steady advancing dynamics given by the temperature-dependent critical velocity.

Quantitatively, experiments showed a power-law dependence of $U^* = c\Delta T^\chi$, with the exponent $\chi = 1$ in de Ruiter et al. [15] and $\chi \simeq 2.65$ in Herbaut et al. [17]. Let us remark that this discrepancy in the values of exponents was attributed to the morphological differences of the solid front: isotropic in de Ruiter et al. [15] and dendritic in Herbaut et al. [17] (see also [30]). Furthermore, the two experimental studies were carried out under different conditions of wettability. Our model rather predicts $\chi = \frac{3}{5}$, see equation (19). Though, a common point between these studies is that the criterion for pinning and unsteady dynamics, is based on a critical temperature in the vicinity of the triple – or here quadruple – line, and that this criterion comes from the phenomenon of kinetic undercooling [15,17].

Still, for the realistic values taken for b, our model captures a good order of magnitude for the critical velocity. In order for the model to be more quantitatively predictive, and inspired by the approach of Schiaffino and Sonin [16], one has to choose b as being temperature-dependent. Figures 4a and 4b indeed suggest such a dependence, i.e. that b should decrease with ΔT in order to get a better agreement between experiments and theory. Hence, we plotted the value of b obtained for the best fit of our model with two series of experimental data of U^* versus ΔT^* with hexadecane from de Ruiter et al. and Herbaut et al. [15,17]. The plot in Figure 6 shows that the value of b decreases with ΔT and is roughly compatible with a power-law of exponent $-3/2$. Still, in the absence of direct measurements of b, we are unable to comment further.

Let us now reconsider the physical meaning of this critical velocity U^*, calculated from the minimal value of θ_L versus U (see Fig. 3). In experiments, a steady situation is observed when $U > U^*$, so that the solid/liquid front remains at some distance from the contact-line. Hence, the situation of a quadruple line shown in Figure 3 can be envisioned in two peculiar situations:

- the spreading of a liquid at an advancing velocity U slightly larger than U^*, so that the solid front remains at very short distance, of the order of a few molecular lengths, to the triple line. This situation prevents the solid front to catch the contact line, which would lead to an additional pinning force and to a dynamics of stick-slip [17]. As $U \gtrsim U^*$, the front advances faster than the spreading and the dynamics turns unsteady. In this sense, our model describes a situation *at the limit of pinning*, in analogy with the *limit of sliding* in solid friction [28,29];

- the spreading of a liquid on its own previously formed solid, on a cold substrate, enabling the growth of the solid-liquid front together with - and toward a direction normal to - the liquid spreading. To the best of our knowledge, this situation was investigated experimentally only in [13].

We come back to an initial assumption that the radius of curvature of the solid front remains smaller than the value of b, which allowed to apply the usual equations of hydrodynamics of wetting on a straight solid. According to equation (15), an order of magnitude for the radius of curvature of the solid-front is obtained from a simple derivation: $r_c \simeq 2r^{3/2}\left(\frac{\rho LU}{\kappa \Delta T}\right)^{1/2}$. As our assumption is $r_c > b$, we evaluate the ratio $\frac{r_c}{b}$ for $r = b$, and we find $\frac{r_c}{b} \simeq 2\left(\frac{b\rho LU}{\kappa \Delta T}\right)^{1/2}$. With the experimental values of hexadecane, and the values of b giving the best fit for corresponding ΔT and U, we find: $\frac{r_c}{b} \simeq 4$ for $\Delta T = 10°$ (taking $b = 0.25$ μm) and $\frac{r_c}{b} \simeq 9$ for $\Delta T = 2°$ (taking $b = 3$ μm), see Figure 4. Therefore, our assumption can be considered as roughly valid, and the corrections due to solid curvature should be negligible, although a more detailed calculation should take these second-order terms into account. In any cases, the curvature of the front is far too weak to induce a shift in the freezing temperature via the so-called Gibbs-Thomson effect.

2.3.2 Critical angle and the offset in ΔT

Figure 5 shows that the model, namely equation (20), provides qualitative agreement with existing experiments, namely those of Tavakoli et al. [14] and of de Ruiter et al. [15]. Those from Herbaut et al. were excluded because they were obtained in different conditions of wetting, namely with a surface treatment which achieved partial wetting conditions with hexadecane and pentadecane.

Still, experimental data points seem to show an offset in temperature, roughly equal to $\Delta T_c = 2.46°$, below which the angle of arrest was not measurable. This offset does not appear in Herbaut et al.'s experiments, which are conducted in a permanent regime and where a solid front always exists within the liquid bridge [17]. Figure 5b indeed shows a better agreement between the model and experiments. Indeed, it could be possible that for low ΔT the stability of supercooled liquid is sufficiently high to allow a characteristic time of nucleation larger than for experiment of single drop unsteady spreading (unsteady states) [14,15] but not in steadily driven liquid bridges [17]. In both cases, the agreement with experiments is improved if b is made temperature-dependent.

3 Conclusion: limitations and prospectives

A model of quadruple line advancing at steady velocity U, which combines hydrodynamic lubrication with solidification in a weakly curved wedge, and calculated between microscopic and mesoscopic cut-off lengths, offers a fair qualitative agreement with experiments of advancing solidifying contact-lines, concerning the prediction of a condition for arrest (pinning). In practice, this can be related to the transition between continuous and stick-slip dynamics occurring under a temperature-dependent threshold velocity. Analytical solutions of the models predict power-laws relating arrest angle θ_a with undercooling ΔT, as well as for the critical velocity U^* with ΔT.

However, the model predictions are questionnable in two points:

- the exponents are different from those deduced from drop spreading experiments. Still, when one allows an adjustable parameter, the cut-off length b, to become temperature-dependent - a possibility emphasized in Schiaffino and Sonin's theoretical approach, the agreement between θ_a, U^* and ΔT becomes quantitatively better. The physical significance of these cut-off length values and their dependence on ΔT, although falling within a range of values which are physical sound, remains unexplained;

- an offset (or threshold) value for the undercooling ΔT has to be introduced in order to fit correctly experimental data of the critical angle of arrest. This threshold, of relatively small magnitude, could be explained by a slight supercooling effect, which prevents the appearance of solidification germs close to the melting point. Indeed, such an offset does not appear when one reaches a permanent regime of spreading with constant driving velocity [17], as a solid phase continuously exists nearby the contact-line.

Despite these limitations, our model predicts a criterion for pinning based on a critical spreading velocity, which is temperature dependent. The geometry of quadruple line also suggests possible experiments mimicking this situation as, for instance, the spreading of a liquid drop on its own solid. We hope this will motivate further studies in the field.

References

1. D. Bonn, J. Eggers, J. Indekeu, J. Meunier, E. Rolley, Rev. Mod. Phys. **81**, 739 (2009)
2. J.H. Snoeijer, B. Andreotti, Annu. Rev. Fluid Mech. **45** (2013)
3. T.D. Blake, J. Colloid Interface Sci. **299**, 1 (2006)
4. G. Berteloot, C.T. Pham, A. Daerr, F. Lequeux, L. Limat, EPL **83**, 14003 (2008)
5. J. Eggers, L.M. Pismen, Phys. Fluids **22**, 112101 (2010)
6. O. Carrier, N. Shahidzadeh-Bonn, R. Zargar, M. Aytouna, M. Habibi, J. Eggers, D. Bonn, J. Fluid Mech. **798**, 774 (2016)
7. F. Doumenc, B. Guerrier, Eur. Phys. J. Special Topics **219**, 25 (2013)
8. E. Rio, A. Daerr, F. Lequeux, L. Limat, Langmuir **22**, 3186 (2006)
9. G. Berteloot, A. Daerr, F. Lequeux, L. Limat, Chem. Eng. Process. Process Intensification **68**, 69 (2013)
10. H. Bodiguel, F. Doumenc, B. Guerrier, Langmuir **26**, 10758 (2010)
11. G. Jing, H. Bodiguel, F. Doumenc, E. Sultan, B. Guerrier, Langmuir **26**, 2288 (2010)
12. S. Schiaffino, A.A. Sonin, Phys. Fluids **9**, 3172 (1997)

13. S. Schiaffino, A.A. Sonin, Phys. Fluids **9**, 2217 (1997)
14. F. Tavakoli, S.H. Davis, H.P. Kavehpour, Langmuir **30**, 10151 (2014)
15. R. De Ruiter, P. Colinet, P. Brunet, J.H. Snoeijer, H. Gelderblom, Phys. Rev. Fluids **2**, 043602 (2017)
16. S. Schiaffino, A.A. Sonin, Phys. Fluids **9**, 2227 (1997)
17. R. Herbaut, P. Brunet, L. Limat, L. Royon, Phys. Rev. Fluids **4**, 033603 (2019)
18. M. Vaezi, H. Seitz, S.F. Yang, Int. J. Adv. Manu. Technol. **67**, 1721 (2013)
19. W.A. Cooper, W.R. Sand, D. Veal, M. Politovich, J. Aircr. **21**, 708 (1984)
20. R.D. Deegan, O. Bakajin, T.F. Dupont, G. Huber, S.R. Nagel, T.A. Witten, Nature **389**, 827 (1997)
21. G. Berteloot, A. Hoang, A. Daerr, H.P. Kavehpour, F. Lequeux, L. Limat, J. Colloid Interface Sci. **370**, 155 (2012)
22. A.G. Marin, O.R. Enriquez, P. Brunet, P. Colinet, J.H. Snoeijer, Phys. Rev. Lett. **113**, 054301 (2014)
23. R. De Ruiter, L. Royon, J.H. Snoeijer, P. Brunet, Soft Matter **14**, 3096 (2018)
24. O. Voinov, Fluid Dyn. **11**, 714 (1976)
25. C.A. Knight, Philos. Mag. **23**, 153 (1971)
26. S.H. Davis, *Theory of solidification* (Cambridge University Press, 2001)
27. R.V. Craster, O.K. Matar, Rev. Mod. Phys. **81**, 1131 (2009)
28. F. Heslot, T. Baumberger, B. Perrin, B. Caroli, C. Caroli, Phys. Rev. E **49**, 4973 (1994)
29. T. Baumberger, C. Caroli, Adv. Phys. **55**, 279 (2006)
30. M. Glicksman, M. Koss, E. Winsa, Phys. Rev. Lett. **73**, 573 (1994)